Paper No:133
A3/B3 Colloquium 2023
PS No. PS3

Enhancement of Electrical Insulation Performance using FGM Techniques in Air Insulated HV GIS

Kenji OKAMOTO
Fuji Electric Co., Ltd.

Hidetaka MASUI
Fuji Electric Co., Ltd.

Hironori YANASE
Fuji Electric Co., Ltd.

Naoki HAYAKAWA
Nagoya University

Katsumi KATO
N. I. T., Niihama College

Hitoshi OKUBO
Aichi Institute of Technology

Masahiro KOZAKO
Kyushu Institute of Technology

Naoki OSAWA
Kanazawa Institute of Technology

Tomohiro INOUE
Nagase Chemtex Co.

Kazuo ADACHI
Central Research Institute of Electric Power Industry

Japan
okamoto-kenji@fujielectric.com

SUMMARY

By applying the permittivity (ε)-functionally graded materials (ε-FGM) technique, the authors have achieved, so far an actual-size insulation spacer with a 30% reduction in diameter compared to that used in conventional 245 kV class SF_6 gas insulated switchgears (GIS) and gas insulated transmission line (GIL).

In this paper, based on the next step of the development, we advanced the ε-FGM techniques under SF_6 alternative gas conditions. We examined the effect of ε-FGM on flashover voltage (FOV) improvement in dry air, which is one of the promising alternative gases to SF_6. As a result in dry air, the lightning impulse (LI)-FOV of the ε-FGM spacer was surely increased being 19% higher at 0.5 MPa-abs and 27% higher at 0.6 MPa-abs than that of the uniform permittivity spacer. These results confirm that the ε-FGM techniques can significantly improve the FOV even in dry air due to its electric field control effect, and expecting to definitely suppress the increase of insulation gap distance and gas pressure, and can strongly contribute to the compactness of SF_6 alternative HV equipment.

KEYWORDS

Gas insulated switchgear (GIS), Insulating Spacer, ε-Functionally Graded Materials (ε-FGM), Dry-Air, Electrical insulation

1 Introduction

In previous studies, by applying the permittivity (ε)-functionally graded materials (ε-FGM) technique, the authors achieved an actual-size insulation spacer with a 30% reduction in diameter compared to that used in conventional 245 kV class SF_6 gas insulated switchgears (GIS) and gas insulated transmission lines (GIL) [1]. In this paper, by applying FGM technology [2]-[6], firstly the permittivity grading distribution in solid insulating spacer was optimized by an inverse calculation technique using a newly developed electric field analysis method. The calculation results shows that the maximum electric field stress of ε-FGM spacer was found to be decreased to 0.74 a.u. compared to that of conventional uniform spacer. Then, a full-scale actual-size ε-FGM spacer with a distributed permittivity from 4.0-10.0 using $SrTiO_3$ and SiO_2 fillers in epoxy insulator was fabricated, and it was experimentally verified the lightning impulse flashover voltage (LI-FOV) in SF_6 gas in the gas-pressure range of 0.3 to 0.6 MPa-abs. As the result, the average LI-FOV was significantly improved by 21% at 0.5 MPa-abs. In addition, it was verified that the withstand voltage tests specified in the IEC62271 standard were fully satisfied and that the long term AC V-t characteristics were also sufficient. The insulating spacers with a 30% smaller diameter for 245kV class GIS has successfully developed using the ε-FGM techniques. The application of the technology is highly effective for downsizing of GIS and GIL [1],[7],[8].

Meanwhile, since SF_6 has a very high global warming potential of 25,200, its use will be restricted in the future, and the application of alternative SF_6 gases is an issue to be addressed as soon as possible. In particular, dry air, which has zero global warming potential and is easy to handle and operation, is already used in GIS and GIL [9]-[12] as an alternative gas to SF_6. Therefore, we examined the effect of ε-FGM on FOV improvement in dry air.

2 Insulation design of actual-size cone-type ε-FGM spacer

For ε-FGM, an actual-size cone-type insulating spacer of GIS was fabricated. The permittivity distribution of the ε-FGM spacer was optimized by an inverse calculation technique using a newly developed electric field analysis method [8]. Figure 1 shows the cross section of the actual-size cone-type FGM spacer. The outer diameter of the HV conductor was 90 mm, and the inner diameter of the grounded tank was 240 mm. The configuration of the grounded tank around the spacer was modified considering the actual GIS spacer.

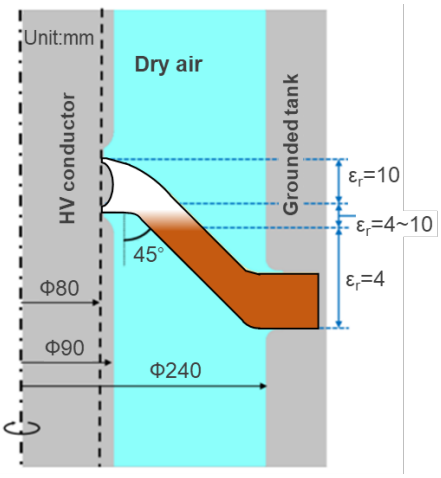

Figure 1: Actual-size cone-type spacer model in air insulated GIS.

The relative permittivity (ε_r) is reduced in six steps, from ε_r = 10 around the HV conductor to ε_r = 4 around the grounded tank. Figure 2(a) shows the electric field distribution around the conventional uniform spacer with the same configuration as the FGM spacer and a constant ε_r = 4, whereas Figure 2(b) shows the electric field distribution around the FGM spacer in Figure 1. The electric field stress at the shield edge of the HV conductor on the concave side of the uniform spacer is defined as 1.0 a.u., which is higher than those on the coaxial HV conductor and spacer surface on the concave and convex sides. In contrast, the electric field stress at the same point of the FGM spacer is reduced to 0.74 a.u., which is 26 % lower than that of the uniform spacer and almost equivalent 0.77 a.u. on the coaxial HV conductor. The electric field strength on the spacer surface on the convex side of the uniform spacer is increased from 0.50 a.u. to 0.73 a.u., which implies that the electric field distribution in SF_6 gas around the FGM spacer is equalized owing to its permittivity distribution.

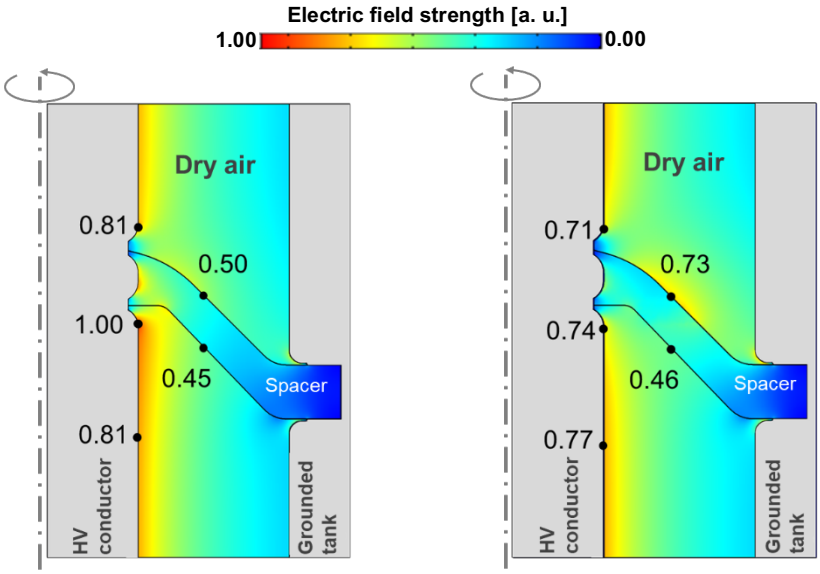

(a) Uniform spacer (b) FGM spacer

Figure 2: Calculated electric field distribution.

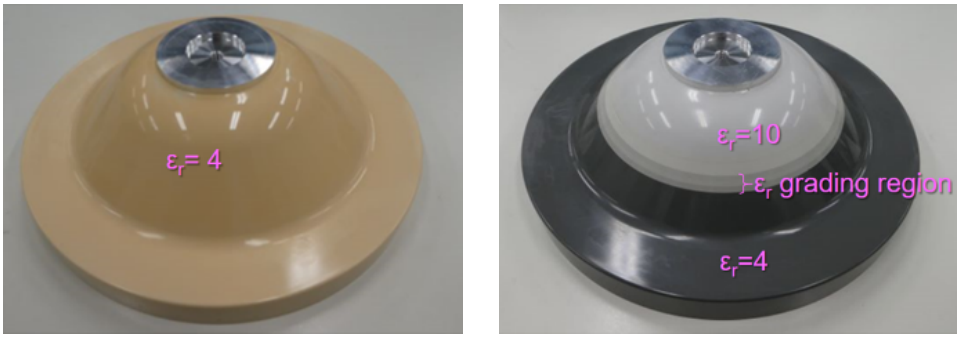

(a) Uniform spacer (b) FGM spacer

Figure 3: Fabricated actual size cone-type spacer.

3 Fabrication of actual-size cone-type FGM spacer

As shown in Table I, two types of composite materials were prepared in advance: a $SrTiO_3$ filler (ε_r = 332) containing a high-permittivity composite material and a SiO_2 filler (ε_r = 4) containing a low-permittivity composite material. By changing the ratio of these two types of composite materials and mixing them, the permittivity distribution was changed, and by casting them into a mold sequentially, a cone-type FGM spacer with permittivity graded from ε_r = 10 to ε_r = 4 was produced.

Table I: Specifications of filler materials in insulation spacer.

Filler material	$SrTiO_3$	SiO_2
Mean diameter	1.0-1.5μm	1.5μm
Relative permittivity	332	4

Figure 3(a) shows a uniform spacer of ε_r = 4, and Figure 3(b) shows a FGM spacer of ε_r = 10-4. In Figure 3(b), the white color region corresponds to ε_r = 10, the black color region corresponds to ε_r = 4, and the gray color region between them is a permittivity graded part.

4 Lightning Impulse flashover (LI-FO) test

Figure 4 show the LI flashover voltage measuring apparatus for actual size insulating spacer. The fabricated cone-type spacer was installed in the pressure tank filled with dry-air at 0.3-0.6 MPa-abs and exposed to negative standard LI voltage. One uniform spacer and one FGM spacer were used in the test. It was measured three times at each pressure. The applied peak voltage started at approximately 0.5 a.u., denoted by an arbitrary unit.

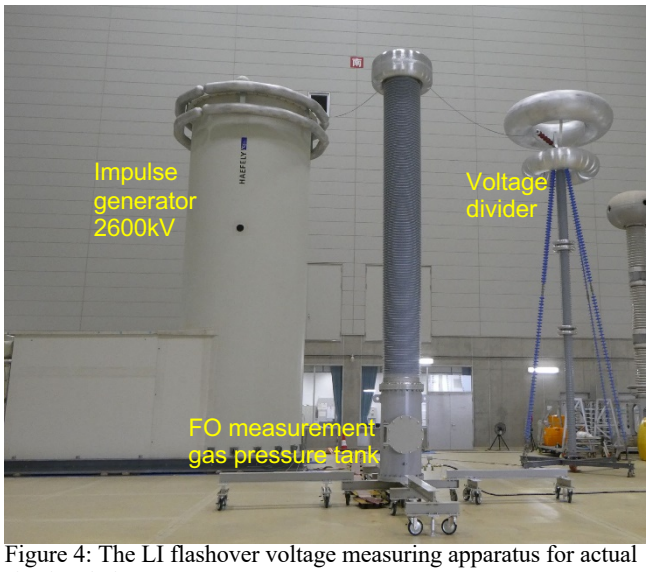

Figure 4: The LI flashover voltage measuring apparatus for actual size insulating spacer.

5 LI-FOV test results and discussion

The cross symbols in Figure 5 show the measured FOV of uniform spacer(black) and FGM spacer(red) as a function of dry air gas pressure. At 0.6MPa-abs, the FGM spacer showed flashover in the range of 1.81 to 1.88a.u., whereas the uniform spacer showed flashover in the range of 1.44 to 1.50 a.u. At 0.5 MPa-abs, the FGM spacer showed flashover in the range of 1.50 to 1.63 a.u., whereas the uniform spacer showed flashover in the range of 1.25 to 1.31 a.u.. Thus, it was experimentally verified that the FOV of the FGM spacer increased more than that of the uniform spacer between 0.3 and 0.6 MPa-abs, and the average of the FOV increase by FGM application was 27% higher at 0.6 MPa-abs and 19% higher at 0.5 MPa -abs. The dotted lines show their approximated curve.

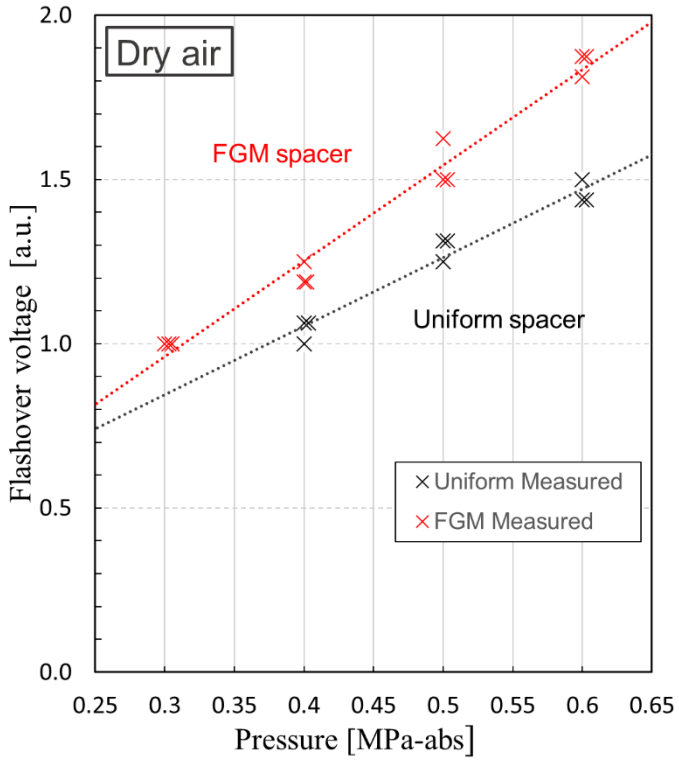

Figure 5: LI flashover voltage of uniform and ε -FGM spacer models in dry air under 0.3 - 0.6MPa-abs.

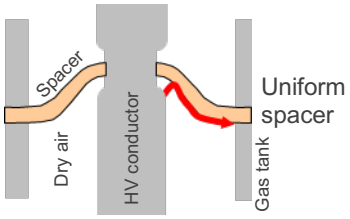

(a) Uniform spacer (Shield edge of HV conductor and spacer surface).

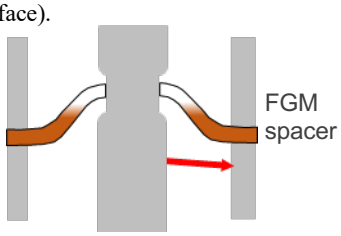

(b) FGM spacer (HVconductor and grounded tank)

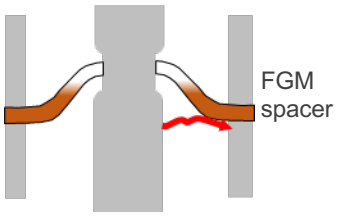

(c) FGM spacer (HV conductor and spacer surface)

Figure 6: LI Flashover trace of cone-type spacers.

The flashover characteristics are discussed in terms of the flashover traces. Figure 6 shows the flashover traces of the uniform spacer and the FGM spacer. The flashover traces of the uniform spacer in Figure 6(a) were started at the shield edge of the HV conductor on the concave side of spacer, which corresponds to the maximum point of the electric field stress in Figure 2(a), as well as on the spacer surface on the concave side of spacer. On the other hand, as shown in Figures 6 (b) and (c), there were two types of discharge patterns for the FGM spacer: discharge from the concave-side coaxial HV conductor to the ground tank and discharge from the coaxial HV conductor shield edge to the spacer surface near the ground tank. The flashover characteristics are exactly the same as in the case of SF_6 [1].

These results suggest that the flashover of the uniform spacer was a surface discharge originating from the shield edge, whereas the flashover of the FGM spacer was a gap discharge between the coaxial cylindrical electrodes.

Figure 7 shows the value converted from the FOV to the flashover electric field stress (FOE). The FOE of the uniform spacers is slightly higher than that of the FGM spacers, although it is approximately equivalent. This is because the high-voltage conductor is the origin of the discharge in both cases. The reason why the FOE of the FGM spacer is slightly lower than that of the uniform spacer, which is considered to have affected of the area effect due to the large high electric field region.

Consequently, the fabricated cone-type actual size FGM spacer exhibited a flashover voltage improvement effect even in dry air, compared with the uniform spacer, owing to the electric field grading and equalization by the FGM spacer.

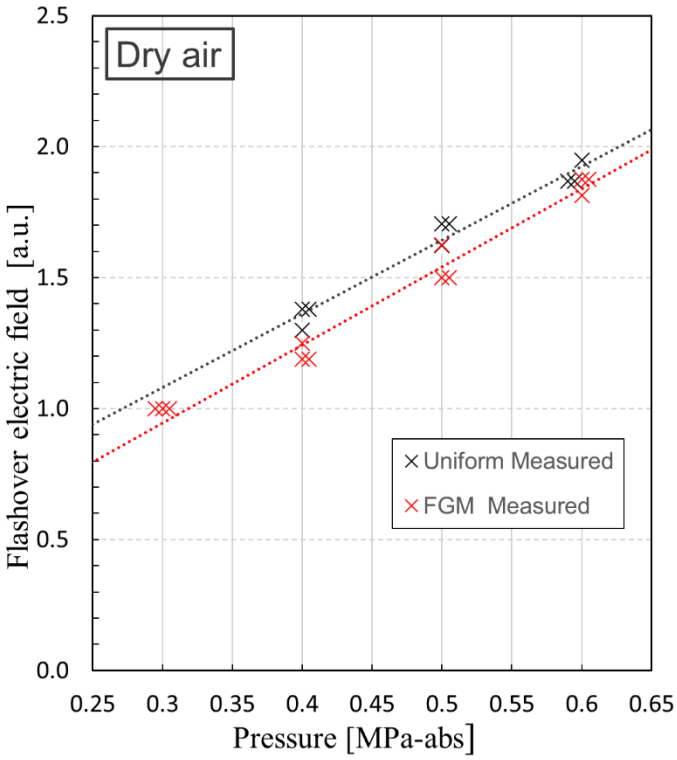

Figure 7: LI flashover electric field stress of uniform and ε -FGM spacer models in dry air.

6 Conclusions

In the case of SF_6 alternative gas, especially natural gas (dry air) has low insulation performance, so it is necessary to increase the diameter of insulating spacers and the filling gas pressure, and the equipment size is estimated to be 1.2-1.5 times larger, which becomes a critical problem to be solved.

However, by applying ε-FGM technology to GIS insulation spacer, it is possible to avoid the increase of insulation gap distance and extra gas pressure, and upsizing of equipment. In particular, it is expected to contribute to the replacement of narrow-area substations (Indoor, underground, mountain side, offshore, etc.) that require the same scale.

This work was supported by the Innovation Program for Energy Conservation Technologies (JPNP12004) of the New Energy and Industrial Technology Development Organization (NEDO).

Bibliography

[1] K. Okamoto, N. Hayakawa, M. Hikita, H. Okubo, K. Kato, N. Osawa. “Development of Sophisticated Cone-Type Insulating Spacer for 245 kV Class GIS by Functional Insulating Materials”, CIGRE Paris Session, D1-10648, 2022.

[2] K. Kato, K. Kimura, S. Sakuma and H. Okubo, “Functionally Gradient Material (FGM) For GIS Spacer Insulation”, 12th International Symposium on High Voltage Engineering (ISH), vol. 2, pp.401-404, 2001.

[3] K. Kato, M. Kurimoto, H. Adachi, S. Sakuma and H. Okubo, “Impulse Breakdown Characteristics of Permittivity Graded Solid Spacer in SF_6”, IEEE Conference on Electrical Insulation and Dielectric Phenomena (CEIDP), pp.401-404, 2001.

[4] H. Okubo, H. Shumiya, M. Ito and K. Kato, “Insulation Performance of Permittivity Graded FGM (Functionally Graded Materials) in SF_6 Gas under Lightning Impulse Conditions”, Conference Record of the 2006 IEEE International Symposium on Electrical Insulation (ISEI), IEEE, pp.332-335, 2006.

[5] H. Okubo, H. Shumiya, M. Ito and K. Kato, “Optimization Techniques on Permittivity Distribution in Permittivity Graded Solid Insulators”, Conference Record of the 2006 IEEE International Symposium on Electrical Insulation (ISEI), IEEE, pp.519-522, 2006.

[6] H. Okubo, K. Kato, N. Hayakawa, M. Hanai and M. Takei, “Functionally Graded Materials and their Applications to High Electric Field Power Equipment”, CIGRE SC D1 – Colloquium in Hungary Budapest, 2009.

[7] N. Hayakawa, K. Kato, H. Okubo, H. Hama, Y. Hoshina and T. Rokunohe, “Electric Field Grading Techniques in Power Apparatus Using Functional Materials”, CIGRE Paris Session, D1-309, 2014.

[8] K. Kato, H. Kojima, N. Hayakawa, H. Mitsudome, H. Yanase, K. Okamoto and H. Okubo, “Inverse Analysis of Permittivity Distribution of FGM (Functionally Graded Materials) Insulator in Gaseous Insulation System”, 21th International Symposium on High Voltage Engineering (ISH), 2019.

[9] M. Kuschel. L.-V. Badicu, J. Christian, M. Kieper, K. Kunde, U. Prucker, J. Riedl, “First F-gas-free and climate-neutral insulated 420 kV GIS busducts installation at TransnetBW”, CIGRE Paris Session, B3-1082, 2022.

[10] T. Uchii, D. Yoshida, S. Tsukao, K. Taketa, K. Tsuboi, “Recent Development of SF6 Alternative Switchgear Using Natural-Origin Gases in Japan”, CIGRE Paris Session, A3-10643, 2022.

[11] N. Nakamura, S. Tsukao, T. Nishioka, K. Taketa, T. Uchii, H. Hama. “Management of SF6 gas leakage from substation equipment and technical guidelines on application of substation equipment using SF6 alternative gases in Japan”, CIGRE Paris Session, B3-10736, 2022.

[12] CIGRE Technical Brochure, No.730, “DRY AIR, N_2, CO_2 AND N_2/SF_6 MIXTURES FOR GAS INSULATED SYSTEMS”, 2018.